ASEAN
Journal of Scientific and Technological Reports
Online ISSN:2773-8752

Research article

Investigating the Performance of Metering Methods in Managing Unbalanced Roundabouts Using VISSIM

Mahbub Hassan[1], An Hong Ki[2*], Hridoy Deb Mahin[3], Abdullah Al Nafees[4], Saikat Sarkar Shraban[5], and Arpita Paul[6]

[1] Faculty of Civil Engineering & Technology, Universiti Malaysia Perlis (UniMAP), Malaysia
[2] Faculty of Civil Engineering & Technology, Universiti Malaysia Perlis (UniMAP), Malaysia
[3] School of Applied Sciences & Technology, Shahjalal University of Science and Technology (SUST), Bangladesh
[4] School of Applied Sciences & Technology, Shahjalal University of Science and Technology (SUST), Bangladesh
[5] School of Applied Sciences & Technology, Shahjalal University of Science and Technology (SUST), Bangladesh
[6] School of Applied Sciences & Technology, Shahjalal University of Science and Technology (SUST), Bangladesh
* Correspondence: hongkian@unimap.edu.my.

Citation:
Hassan, M.; Ki, H.A.; Mahin, D.H.; Nafees, A.A.; Shraban, S.S.; Paul, A. Investigating the performance of metering methods in managing unbalanced roundabouts using VISSIM. *ASEAN J. Sci. Tech. Report.* **2025**, *28*(2), e255674. https://doi.org/10.55164/ajstr.v28i2.255674

Article history:
Received: August 29, 2024
Revised: December 20, 2024
Accepted: January 30, 2025
Available online: February 23, 2025

Abstract: Unbalanced roundabouts often face higher traffic volumes on certain approaches, leading to congestion and delays. Metering signals can help reduce delays, manage queues, and optimize performance. This study evaluates the effectiveness of metering signals in improving traffic flow at unbalanced roundabouts using VISSIM simulation software. The study focuses on identifying optimal detector placements to minimize delays and queues. Results showed that at 4:30 pm, both the North and West Lanes had LOS F, but after introducing signals at the South Lane and optimizing detector placement at 240 meters, the West Lane improved to LOS D and the North Lane to LOS B. At noon, the West Lane initially had LOS F. Still, with signal control adjustments at the 350-meter detector, it improved to LOS D. Emissions and fuel consumption also decreased in the South and East Lanes, demonstrating that metering signals can significantly enhance roundabout performance. This study was limited by using a student version of VISSIM, which restricted signal control to a 2-stage system.

Keywords: VISSIM; Unbalanced roundabout; Queue length; Traffic signal metering method

1. Introduction

The global urban population is projected to increase from 3.9 billion to 6.3 billion by 2050 [1]. Rapid urbanization has increased transportation, causing traffic, pollution, and delays. Since 2008, over half the global population has lived in urban areas, growing at 1.8% annually [2], and by 2050, over two-thirds will live in cities [3]. The 2023 INRIX Global Traffic Scorecard, published in June 2024, reveals that New York was the most congested urban area, with drivers losing 101 hours to traffic in 2023, costing over $9.1 billion. U.S. drivers lost an average of 42 hours, totaling $70.4 billion, with delays rising in 98 of the top 100 urban areas globally. In the U.K., drivers lost 61 hours, costing £7.5 billion, an 11% increase from 2022. In Germany, drivers lost 40 hours, costing €3.3 billion, a 14% rise from 2022. These figures emphasize the urgent need for effective solutions to reduce congestion and its costs. Traffic congestion in 83 countries causes over 22,000 deaths annually and costs the healthcare system $18 billion annually [4]. The WHO identifies traffic congestion pollution as a major cause of

high mortality in large cities. Around 40 million residents in the 115 largest EU cities are exposed to air quality levels above WHO guidelines [5].

In transportation engineering, "imbalanced flow" occurs when traffic volumes are below a road's capacity, allowing smooth movement. However, delays, queues, and congestion result when flow rates reach or exceed capacity. Many studies have explored the effects of unbalanced flows at roundabouts, a common road intersection type [6–8]. Understanding the impact of suboptimal traffic patterns on roundabouts is key to reducing congestion. While roundabouts help mitigate congestion, they are vulnerable to traffic issues. Fluctuating demands and uneven flow can reduce the spacing between circulating vehicles, making it difficult for vehicles to find safe entry points [6]. Metering systems have been proposed [9] to mitigate congestion from irregular traffic flow. Kangar, a city in Perlis, Malaysia, features the Bulatan Tuanku Syed Putra roundabout, a crucial junction connecting major thoroughfares and vital to transportation efficiency and economic and social cohesion. Traffic flow peaks at 4:30 PM as people return home and at noon on Fridays for mosque prayers.

Metering signals at roundabouts are a modern traffic management technique that regulates flow and creates gaps in the circulating stream. This method helps reduce queuing and delays caused by unbalanced traffic flow and high demand [10, 11]. The primary objective of this research is to evaluate the effectiveness of metering techniques in improving traffic flow at roundabouts under unbalanced conditions. Utilizing VISSIM microsimulation, the study explores optimal detector placements to minimize queues and delays, providing actionable recommendations for engineers, planners, and policymakers.

The paper is organized as follows: Section 2 reviews the literature on urban traffic congestion, roundabouts, traffic flow imbalances, and metering signal strategies. Section 3 outlines the study methodology, including signal deployment, simulation, data collection, software (VISSIM), parameter settings, and tested scenarios. Section 4 presents simulation findings on metering strategies for improving traffic flow and reducing congestion. Section 5 compares results with theoretical expectations and prior studies. Section 6 concludes with key findings and their implications for urban traffic management. Section 7 discusses study limitations, and Section 8 explores future research directions.

2. Literature Review

This literature review examines recent research on the impact and effectiveness of metering signals at unbalanced roundabouts. It focuses on their ability to improve traffic flow, reduce delays, enhance safety, and address implementation challenges. Unbalanced roundabouts with uneven traffic volumes often suffer from congestion and delays. Metering signals offer a solution by regulating vehicle entry from dominant approaches. A metering roundabout uses detectors and traffic signals to coordinate based on queue length. As shown in Fig. 1, the signal turns red when Detector C on the dominant approach reaches a threshold.

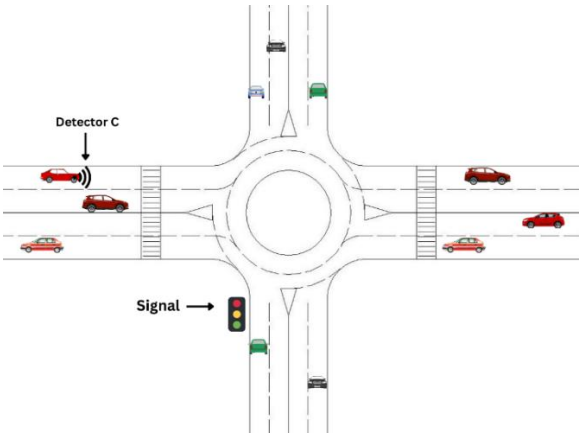

Figure 1. Concept of metering roundabout

Over the years, numerous studies have explored the implementation of metering roundabouts. Most of this research focuses on various signal control methodologies and their effects on traffic dynamics, using microsimulation tools like VISSIM and analytical models such as SIDRA. For instance, Akçelik R [11] used the SIDRA INTERSECTION software to analyze metering roundabouts, showing that shorter cycle times could improve performance compared to current practices. However, the study highlighted the need for real-world testing to validate these analytical results, calling for empirical validation.

Martin-Gasulla M et al. [7, 12] conducted two studies in Valencia, Spain. The first involved field study, calibration, and optimization using surveillance cameras and Vis VAP and VISSIM software, which showed that metering increases capacity under high-flow conditions. However, it wasn't tested in real-world settings. The second used microsimulation with video data, achieving a 60% reduction in delays and a 60% increase in capacity, but it was limited to one-lane roundabouts. Furthermore, Sun, X [13] et al. introduced shockwave and capacity models with sensitivity analysis, suggesting that signalized roundabouts could exceed intersection capacity and that short cycles might benefit intersections. However, it was a preliminary study that required further testing for confirmation.

Duan Y et al. [8] developed a model and simulation-based algorithm for metering signals using headway data and VISSIM software. The study reported a 25.7% reduction in delays with metering signals but focused only on roundabouts, excluding pedestrians and non-motorized vehicles. Similarly, Adegbaju, O. A. [14] showed that traffic signals can improve service (LOS) and reduce delays and queues at intersections through VISSIM simulations. However, the study was limited to specific intersections, highlighting the need for broader studies. In addition, An, H. K et al. [15] used numerical models and drone data calibrated with AIMSUN 7 simulations to reduce delays, queue lengths, and CO_2 emissions. However, the study was limited to two signal phases and a single-lane roundabout.

An, H. K et al. [16] utilized Adaptive Neuro-Fuzzy Inference System (ANFIS) models to predict queue lengths in the Old Belair Road roundabout drone data. Still, they did not consider detector locations for signal adjustments. Osei, K. K. [17] used microsimulation with VISSIM to analyze signalized configurations at two four-leg roundabouts in Ghana. They found that signalization improved capacity and reduced delays despite challenges from high left-turn traffic, necessitating design adjustments for complex traffic patterns. Meanwhile, Vichova, K. et al. [18] evaluated an intersection in the Zlín region of the Czech Republic using PTV VISSIM. They concluded that roundabouts effectively reduce accidents but noted limitations due to visibility issues at the studied intersection.

Another study by An, H. K. et al. [19] on the Old Belair Roundabout in Adelaide used drone footage with MATLAB and AIMSUN software, reducing queue length from 689 to 499 meters. However, it emphasized the need for varied conditions and smarter methods for broader applicability.

In 2023, several studies explored different traffic signal control methods. An, H. K. et al. [9] analyzed three control methods—indirect, part-time, and full control—at the Changwon City Hall roundabout in South Korea using MATLAB and VISSIM. The study achieved a 46.1% reduction in density, a 32.8% reduction in delays, and a 14.8% increase in capacity but recommended more case studies with varied designs. Similarly, Kabit, M. R. et al. [20] studied the microsimulation of roundabout control strategies, including Approach-Signal-Control Roundabout (ASCR), Two-Stop-Line Signalized Roundabout (TSLSR), and partial control signal phasing. They found that partial signals significantly improved LOS but were unsuitable for major reconstructions. Finally, Assolie, A. A. et al. [21] analyzed traffic data from two roundabouts in Amman, Jordan, using Python and VISSIM. The study reduced delays by 85.25% and queue lengths by 76.76% for cars and heavy vehicles. Still, it highlighted the need to include a wider variety of vehicles for a comprehensive understanding of traffic dynamics.

Studies on signal timing show that signalized roundabouts can outperform normal roundabouts under specific conditions. Most research has focused on reducing queues and delays while increasing capacities [9]. Table 1 summarizes recent studies on metering roundabouts, detailing the study area, data source, software used, method, key findings, and limitations.

Table 1. Relevant studies on the metering method

Year	Ref.	Study Area	Data Source	Used Software	Methodology	Findings	Limitations
2023	[9]	Changwon City, South Korea	Traffic volume data	MATLAB, VISSIM	Examined three traffic signal control methods: indirect, part-time, and full control.	Reduced density by 46.1%, delays by 32.8%, increased capacity by 14.8%	It needs more case studies with varied designs
2023	[20]	Malaysia	Traffic data	VISSIM	Microsimulation of ASCR, TSLSR, and partial control signal phasing	ASCR is unsuitable, TSLSR shows minor improvements, partial signals significantly improve LOS	Not suitable for major reconstructions
2023	[21]	Amman City, Jordan	Traffic data	Python, VISSIM	Analyzed roundabout data	Reduced delays by 85.25%, queue length by 76.76%	Focuses on cars and heavy vehicles only
2022	[19]	Adelaide, South Australia	Drone footage data	MATLAB, AIMSUN	Data collection and optimization	Reduced queue length from 689 to 499 m	It needs varied conditions and smarter methods.
2021	[18]	Zlín Region, Czech Republic		VISSIM	Analysis, induction, comparison, simulation	Roundabout eliminates intersection accidents	Limited to one intersection with visibility issues
2021	[17]	KNUST police station and Ejisu Municipal, Ghana	Traffic volume, intersection geometry, queue length, travel time	VISSIM	Microsimulation of signalized configurations	Signalization improved capacity and reduced delays	High left-turn traffic blocks through lanes
2019	[16]	Adelaide, South Australia	Drone data	MATLAB	ANFIS models to predict queue lengths, compared with drone data	ANFIS effectively predicts queue lengths	It does not consider detector locations for signal adjustments

Table 1. Relevant studies on the metering method

Year	Ref.	Study Area	Data Source	Used Software	Methodology	Findings	Limitations
2018	[8]	Olsen Avenue, Queensland, Australia.	Headway data	VISSIM	Model and simulation-based algorithm for metering signals	Delay reduction of up to 25.7% with metering signals	Excludes pedestrians and non-motorized vehicles; focuses only on roundabouts
2018	[14]	Michigan	Field Data	VISSIM		Traffic signals improve LOS, reduce delays and queues	Focused on specific intersections.
2017	[15]	Adelaide, South Australia	Drone data	AIMSUN	Numerical model with drone data, calibrated with simulations	Reduced delay, queuing length, and CO2 emissions	Limited to two signal phases and one roundabout
2016	[12]	Valencia, Spain	Surveillance camera	Vis VAP, VISSIM	Field study, calibration, and optimization	Metering boosts capacity at high flows	Not tested in real-world conditions
2016	[7]	Valencia, Spain	Video data	Vis VAP, VISSIM	Microsimulation	Delays reduced by 60%, capacity increased by 60%	Limited to one-lane roundabouts
2016	[13]				Shockwave and capacity models, sensitivity analysis	Signalized roundabouts can exceed intersection capacity; short cycles favor intersections.	Preliminary; needs further testing.
2011	[11]	Melbourne, Australia		SIDRA INTERSECTION	Analytical model	Lower cycle times than current practice	Needs real-life testing

The flowchart in Fig. 2 presents a detailed strategy for optimizing roundabout traffic signal operations. It starts with reviewing existing studies and identifying key factors that affect traffic flow. Data was collected through various methods, including drone videos and manual surveys. Initially, the traffic network is simulated without using VISSIM software. Then, a model integrating signals is developed to manage unbalanced traffic flows. After successfully calibrating this model, Python analyzes data and identifies the best locations for traffic detectors. The final step involves exploring the potential benefits of the system.

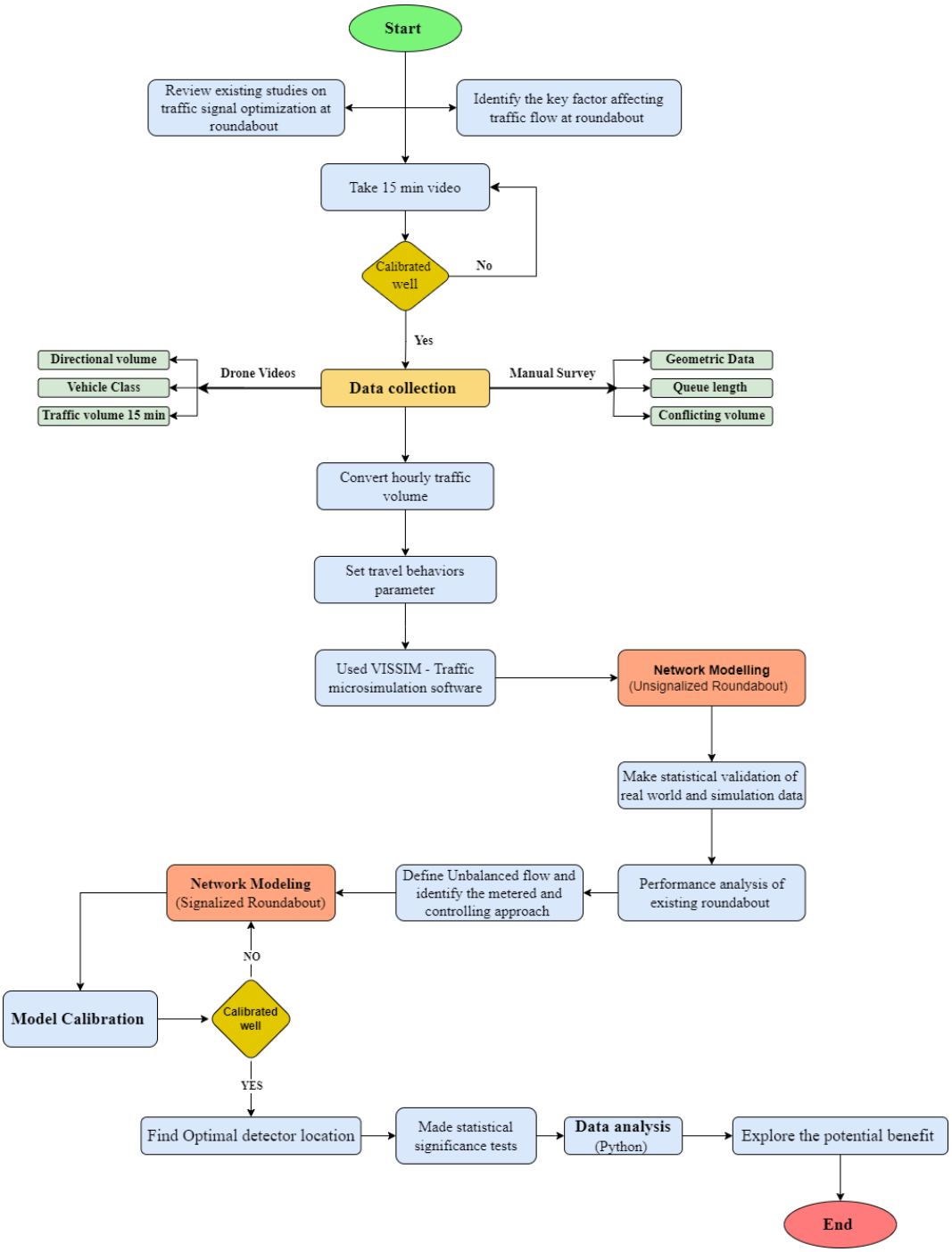

Figure 2. Research framework

3.1 Study site

Kangar, Perlis, Malaysia, benefits from the Bulatan Tuanku Syed Putra roundabout, a key traffic hub that improves transportation efficiency and supports economic growth. Major roads like Jalan Kangar-Alor Setar, Persiaran Jubli Emas, and Jalan Kangar-Padang Besar enhance trade and connectivity, including links to Thailand. Jalan Padang Behor also contributes to regional connectivity.

Traffic imbalances occur in the afternoon due to offices on the west approach, causing congestion and long queues. On Fridays, large gatherings at the Alwi Mosque further contribute to congestion. Fig. 3(a) an extracted map, Fig. 3(b) drone footage during non-peak hours, Fig. 3(c) manual traffic control by police during peak hours, and Fig. 4(d) long queues at the west approach during peak hours.

Figure 3. Study site (a) Selected roundabout from OpenStreetMap (b) Drone footage captured during non-peak hours (c) Manual traffic control by police during peak hours (d) Long queues at the west approach during peak hours

3.2. Data collection procedure

3.2.1 Hourly traffic volume

The data for this research was collected using drone footage of a 15-minute video. From this video, the number of vehicles was determined through manual calculation.

$$PHF = \frac{Peak\ Hour\ Flow\ Rate}{V_{15\ peak} * 4} \quad (1)$$

Subsequently, the 15-minute data was converted to its one-hour equivalent volume. Equations (1) and (2) [22] were used for this conversion. Equation (1) calculates the peak hour factor (PHF). After calculating the PHF, this value is used in equation (2) to calculate the hourly traffic volume.

$$Flow\ rate = PHF * V_{15\ peak} * 4 \quad (2)$$

3.2.2 Temporal distribution of data collection

Data for analysis at the Bulatan Tuanku Syed Putra roundabout was collected on Friday, January 5, 2024, (12:00 to 1:00 PM) and Monday, January 8, 2024 (4:30 to 5:30 PM). High-definition footage from the DJI Mini 3 drone captured traffic flow, vehicle interactions, and congestion points. The data was processed to analyze directional volume, vehicle classifications, and hourly traffic volumes. Manual data collection also included geometric data, queue length, and conflicting volume.

Table 2 shows the directional volume data for each approach, collected between 12:00–1:00 PM and 4:30–5:30 PM. At 12:00–1:00 PM, the total vehicle volume was 3,000, with the West approach having the highest traffic (1,660 vehicles per hour, 55.3%). At 4:30–5:30 PM, traffic increased to 3,550 vehicles per hour, with the West approach still the most congested (1,660 vehicles per hour, 46.8%). The South approach increased to 890 vehicles per hour, accounting for 25.1% of the total volume.

Table 2. Directional Volume

12.00 p.m. scenario				
Approach	Direction	Volume (veh/hr)	Total Volume	Percentage (%) of total Vehicle
SBD [1]	L [5]	101		0.3
	T [6]	131	380	0.3
	R [7]	147		0.4
NBD [2]	L	149		0.3
	T	385	550	0.7
	R	259		0.5
WBD [3]	L	145		0.4
	T	185	410	0.5
	R	80		0.2
EBD [4]	L	447		0.3
	T	754	1660	0.5
	R	460		0.3
Total			3000	
4.30 p.m. scenario				
Approach	Direction	Volume (veh/hr)	Total Volume	Percentage (%) of total Vehicle
SBD	L	319		0.6
	T	147	520	0.3
	R	53		0.1
NBD	L	392		0.4
	T	194	890	0.2
	R	304		0.3
WBD	L	93		0.2
	T	176	480	0.4
	R	211		0.4
EBD	L	344		0.2
	T	817	1660	0.5
	R	498		0.3
Total			3550	

1= south bound direction, 2= north bound direction, 3= west bound direction, 4= east bound direction, 5= Left, 6= Through, 7= Right

Table 3 shows the vehicle data (cars, bikes, buses, and heavy vehicles) from the North, South, East, and West approaches at 12:00 PM and 4:30 PM. At 12:00 PM, cars dominated traffic, with the highest percentage in the West (84.98%), followed by the North (83.24%), South (82%), and East (77.8%). At 4:30 PM, the vehicle distribution remained consistent, indicating stable traffic patterns between the two times. Table 4 presents manually surveyed queue lengths (in meters) for the West, North, East, and South approaches from 12:00 PM–1:00 PM and 4:30 PM–5:30 PM. The West and North approaches had the longest queues at 12:00 PM–1:00 PM. By 4:30 PM–5:30 PM, overall queue lengths decreased, particularly at the North and South approaches, with the East approach showing the most significant reduction.

Table 3. Vehicle class

12.00 p.m. scenario				
Approach	Car (%)	Bike (%)	Bus (%)	Heavy Vehicle (%)
SBD	83.24	15.72	0.1	1.03
NBD	82	16.2	0.1	1.07
WBD	77.8	21.9	0.2	0.1
EBD	84.98	14.34	0.24	0.44
4.30 p.m. Scenario				
Approach	Car (%)	Bike (%)	Bus (%)	Heavy Vehicle (%)
SBD	83.24	15.72	0.1	1.03
NBD	82	16.2	0.1	1.07
WBD	77.8	21.9	0.2	0.1
EBD	84.98	14.34	0.24	0.44

3.2.3 Equipment calibration protocols

It is essential to follow a rigorous calibration protocol to ensure accurate data collection using a drone for traffic monitoring. Begin by calibrating the drone's internal camera parameters using common calibration boards to address image distortion, as discussed by Du et al. [23]. This involves setting up the calibration board at various angles and distances to capture a range of images, which are then used to correct lens distortions and refine camera parameters. Additionally, the drone's external parameters can be calibrated by positioning it at known coordinates and using ground control points to adjust for spatial discrepancies, as demonstrated by Lee [24]. This method ensures that the spatial data captured by the drone aligns accurately with real-world measurements. Implementing these calibration steps enhances the reliability and precision of the traffic data collected, thereby supporting more accurate traffic simulation and analysis.

3.3. Traffic flow analysis

Table 5 outlines the geometric specifications and component locations in the traffic simulation. It shows a link width of 3.5 m and a circular link diameter of 65 m. Data collection points are 9.5 m from the circular link, while queue counters are 8.5 m away. Two 5-m-long rectangular detectors are used for monitoring, and the signal head is positioned 5 m from the circular link to ensure visibility and traffic management efficiency. These parameters optimize the placement and dimensions of key traffic system components.

Table 4. Manually Survey Queue Length

12.00 p.m. scenario				
Time	West(m)	North(m)	East(m)	South(m)
12.00-12.05	728	321	325	431
12.05-12.10	728	1128	325	431
12.10-12.15	736	1122	324	431
12.15-12.20	736	1122	320	425
12.20-12.25	918	321	975	428
12.25-12.30	915	318	518	422
12.30-12.35	910	312	518	416
12.35-12.40	917	306	0	410
12.40-12.45	920	312	0	485
12.45-12.50	925	318	0	480
12.50-12.55	930	320	10	420
12.55-1.00	920	315	15	414
4.30 p.m. scenario				
Time	West(m)	North(m)	East(m)	South(m)
4.30-4.35	92	36	28	90
4.35-4.40	136	84	23	192
4.40-4.45	130	77	18	200
4.45-4.50	125	72	15	200
4.50-4.55	317	191	12	208
4.55-5.00	319	193	42	184
5.00-5.05	310	187	40	187
5.05-5.10	321	430	95	185
5.10-5.15	316	433	90	180
5.15-5.20	320	429	94	184
5.20-5.25	318	425	88	181
5.25-5.30	315	419	93	185

Table 5. Geometric Specifications of Roundabout

Direction	Entry Lane		Exit Lane		Circulatory Lane	
	No. of Lanes	Lane Width (m)	No. of Lanes	Lane Width (m)	No. of Lanes	Lane Width (m)
SBD	2	3.50	2	3.50	2	3.50
NBD	2	3.50	2	3.50	2	3.50
WBD	2	3.50	2	3.50	2	3.50
EBD	2	3.50	2	3.50	2	3.50

Unbalanced flow in roundabouts is evaluated using the circulating traffic ratio (ρi). A balanced approach is characterized by ρi = 0.5, indicating that the circulating traffic consists of 50% from the first upstream approach—defined as the initial entry point where vehicles merge with circulating traffic—and 50% from the second upstream approach [25]. Conversely, an unbalanced approach, where ρi = 0 or 1, signifies that all circulating traffic originates exclusively from the first upstream approach. The definition of the unbalanced flow is shown in Fig 4.

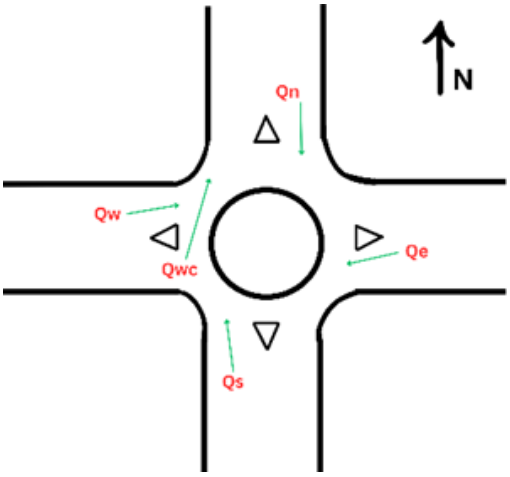

Figure 4. Traffic flow analysis at the roundabout

$$\rho_w = \frac{Q_{sw}}{Q_{sw} + Q_{ew} + Q_{nw}} = \frac{Q_{sw}}{Q_{wc}} = \frac{161}{181} = 0.89 \quad (3)$$

$$\rho_w = \frac{Q_{sw}}{Q_{sw} + Q_{ew} + Q_{nw}} = \frac{Q_{sw}}{Q_{wc}} = \frac{498}{709} = 0.70 \quad (4)$$

Here,

- Q_{sw} = traffic from south passing West
- Q_{ew} = traffic from east passing west
- Q_{nw} = traffic from north passing West
- $Q_{wc} = Q_{sw} + Q_{ew} + Q_{nw}$

For both the 12.00 PM and 4:30 PM scenarios, equations (3) and (4) indicate that the West approach is the controlling approach due to its high total volume of vehicles. The South approach, which has a significant total volume and high through traffic, shows a circulating traffic ratio ($\boldsymbol{\rho}_w$) of 0.89 for the 12 PM scenario and 0.70 for the 4:30 PM scenario. These ratios indicate an unbalanced flow, with traffic patterns heavily influenced by upstream traffic in each scenario.

3.5 Vehicle behavior parameters

Table 6 below shows the car-following, lane-changing, awareness, and aggressiveness parameters used for simulating the roundabout in the VISSIM software.

Table 6. Vehicle behavior parameters

Car Following Parameters		Lane Changing Parameters	
CC0 (Standstill Distance)	2.0 m	Maximum Deceleration for Cooperative Braking	4.5m/s²
CC1 (Headway Time)	1.3 sec	Safety Distance Reduction Factor	0.7
CC2 (Following Variation)	4.0 m	Maximum Deceleration for Own Braking	3.0m/s²
CC3 (Threshold for Entering 'Following')	-8.0 m	Accepted Deceleration for Lane Change	2.5m/s²
CC4 (Negative Following Threshold)	-0.35	Waiting Time Before Diffusion	45sec
CC5 (Positive Following Threshold)	0.35	Emergency Stopping Distance	5m
CC6 (Speed Dependency of Oscillation)	11	Aggressiveness And Awareness	
CC7 (Oscillation Acceleration)	0	Aggressiveness	40%
CC8 (Standstill Acceleration)	3.0 m/s²	Awareness	90%
CC9 (Acceleration At 80 Km/H)	1.2 s/s²		

3.6 Statistical validation of simulation and real-world data

Table 7 compares RMSE values, revealing significant differences in simulation accuracy.

Table 7. Statistical validation of data

12.00 p.m. scenario			
Approach	Volume (veh/hr)		RMSE
	Simulation	Real-world	
SBD	420	380	97.60
NBD	680	550	
WBD	550	410	
EBD	1660	1660	
4.30 p.m. scenario			
Approach	Volume (veh/hr)		RMSE
	Simulation	Real-world	
SBD	660	520	93.27
NBD	990	890	
WBD	540	480	
EBD	1700	1660	

In the 12.00 PM scenario, the RMSE of 97.60 suggests moderate accuracy with notable deviation, indicating areas for improvement. In contrast, the 4:30 PM scenario has an RMSE of 93.27, demonstrating perfect accuracy and successfully replicating real-world data without discrepancies.

3.7 Evaluate the performance of unsignalized roundabout

Fig. 5(a) and (b) clearly show the heavy traffic at the roundabout before a traffic signal was installed, showing a major blockage at the west approach where cars are completely stopped. This occurs because the first car entering the roundabout blocks the west approach, stopping all other cars from moving forward. As a result, the cars behind have to stop and wait for a long time. The more cars that join the queue, the longer the wait becomes. The long queue at the roundabout leads to worsening traffic and driver frustration, with some attempting risky maneuvers. This highlights the roundabout's poor traffic management without a signal.

Table 8. LOS for the vehicular delay (HCM-2017)

Level of service (LOS)	Average delay 'd' (sec/veh)
A	≤ 5
B	6≤d≤15
C	16≤d≤20
D	21≤d≤35
E	36≤d≤65
F	>65

Fig. 5(c) and (d) show the level of service, with Fig. 5(c) showing an F at the west approach and E, C, and D at other approaches, indicating an unbalanced condition. In Fig. 5(d), the West and north approaches have an F, while the others are E and B, also showing an unbalanced condition at 4:30 PM. The level of service is based on the HCM-2017 manual (Table 8).

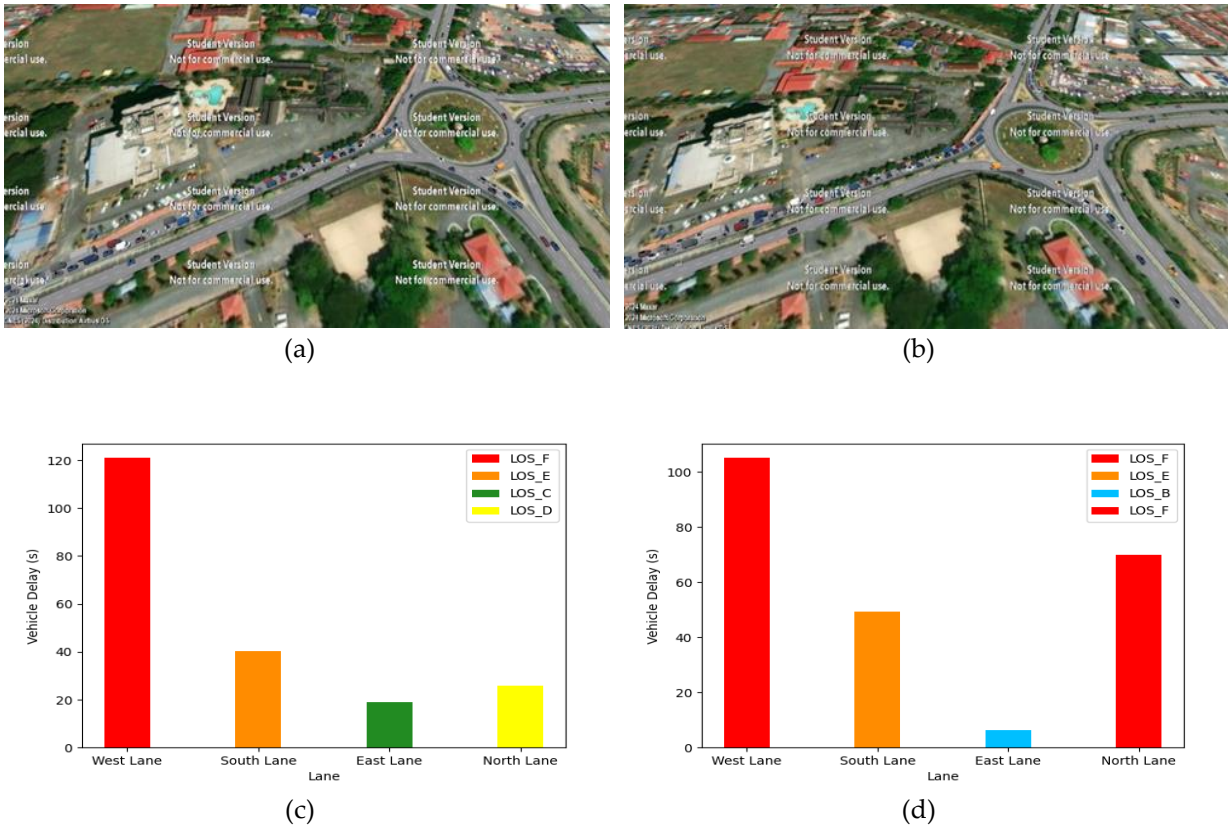

Figure 5. Unbalanced traffic flow at unsignalized roundabout (a) 12 PM Scenario; (b) 4.30 PM Scenario; (c) 12 PM LOS; and (d) 4.30 PM LOS

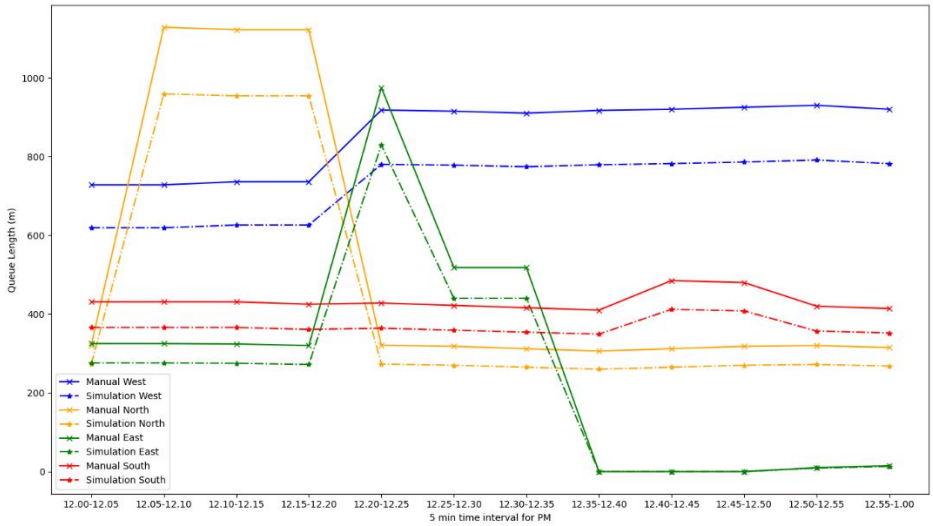

Figure 6. Comparison of simulation and manually collected queue length data of 12.00 PM to 1.00 PM

Fig. 6 compares simulation data with manually collected data. In Fig. 6, from 12:00 PM to 1:00 PM, the West approach had the longest queues, peaking at 930 vehicles, while the North approach peaked at 1,128 vehicles, indicating significant congestion. Fig. 7, for the 4:30 PM to 5:30 PM scenario, shows longer queues on the West and North approaches, with the South approach peaking at 433 vehicles and the North approach at 319 vehicles. These results highlight unbalanced traffic flows, particularly on the North and South approaches, suggesting a need for optimized signal settings to reduce congestion.

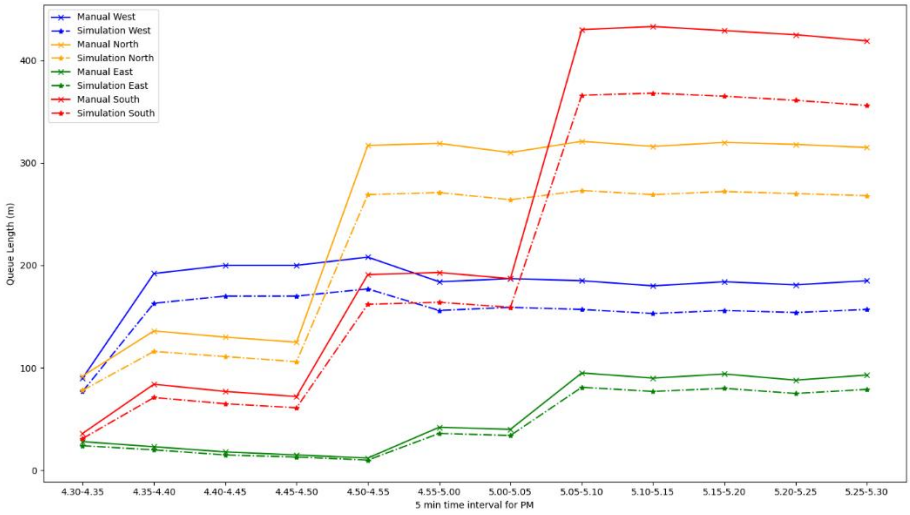

Figure 7. Comparison of simulation and manually collected queue length data of 4.30 PM to 5.30 PM

3.4.1 Detector Placement Locations

To identify the optimum detector location [26] for the 12.00 PM scenario, 10 scenarios were developed and analyzed. The purpose was to evaluate and determine the most effective detector placement for accurate performance. Table 9 presents an overview of these 10 scenarios created and tested during simulation. To determine the optimum detector location [26] for the 4:30 PM scenario, 12 distinct scenarios were designed and analyzed. These scenarios were created to evaluate and identify the most effective placement of the detector for optimal performance during this specific period. Table 10 provides a comprehensive overview of the 12 scenarios tested during the simulation process. Table 10 provides a comprehensive overview of the 12 scenarios tested during the simulation process. In this study, five random-seed samples were randomly selected to obtain unbiased results, and the average value was used.

Table 9. Detector location for 12 PM scenario

No of scenarios	Descriptions
S1	SL[8] is signalized, and a detector is placed 240 m from the stop line on the west lane
S2	SL is signalized, and a detector is placed 250 m from the stop line on the west lane.
S3	SL is signalized, and a detector is placed 260 m from the stop line on the west lane.
S4	SL is signalized, and a detector is placed 270 m from the stop line on the west lane.
S5	SL is signalized, and a detector is placed 300 m from the stop line on the west lane.
S6	S[9] and EL[10] are signalized, and a detector is placed 240 from the stop line on the west lane.
S7	S and EL are signalized, and a detector is placed 250 from the stop line on the west lane.
S8	S and EL are signalized, and a detector is placed 260 from the stop line on the west lane.
S9	S and EL are signalized, and a detector is placed 270 from the stop line on the west lane.
S10	S and EL are signalized, and a detector is placed 300 from the stop line on the west lane.

8= South Lane, 9 = South, 10 = East Lane

Table 10. Detector location for 4.30 PM scenario

No of scenarios	Descriptions
S1	SL is signalized, and a detector is placed 300 m from the stop line on the west lane.
S2	SL is signalized, and a detector is placed 350 m from the stop line on the west lane.
S3	SL is signalized, and a detector is placed 400 m from the stop line on the west lane.
S4	SL is signalized, and a detector is placed 450 m from the stop line on the west lane.
S5	SL is signalized, and a detector is placed 500 m from the stop line on the west lane.
S6	SL is signalized, and a detector is placed 550 from the stop line on the west lane.
S7	S and EL are signalized, and a detector is placed 300 from the stop line on the west lane.
S8	S and EL are signalized, and a detector is placed 350 from the stop line on the west lane.
S9	S and EL are signalized, and a detector is placed 400 from the stop line on the west lane.
S10	S and EL are signalized, and a detector is placed 450 from the stop line on the west lane.
S11	S and EL are signalized, and a detector is placed 500 m from the stop line on the west lane.
S12	S and EL are signalized, and a detector is placed 550 from the stop line on the west lane.

4. Result

4.1 Simulation procedure

This study modeled a roundabout in VISSIM through a detailed process to ensure its accuracy and functionality. The approach involved creating road segments for the roundabout's entry and exit points, followed by connecting these segments to form the roundabout's circular path. Right-of-way rules were established to prioritize vehicles circulating within the roundabout, and conflict areas were incorporated to manage potential collision points. Strategic data collection points were set up around the roundabout to capture traffic volumes, speeds, vehicle types, and queue lengths. These data points provided the necessary information to analyze traffic flow and identify areas for improvement. A 2-stage adaptive traffic signal control system was integrated into the simulation to enhance traffic management. This system used real-time data from a vehicle detector to dynamically adjust the signal timings, helping to optimize traffic flow and reduce congestion. The detector, placed on the west approach, monitored incoming traffic volumes, and the controller on the south approach adjusted signal timings based on the collected data, prioritizing vehicles exiting the west approach. The VISSIM model was further refined through a comprehensive calibration process, where data on traffic flow, vehicle speeds, and queue lengths were gathered during peak and off-peak hours [27]. Key simulation parameters, such as vehicle arrival rates, speeds, and driver behavior, were adjusted to minimize discrepancies between simulated and observed data [28]. The calibration accuracy was quantitatively assessed using statistical measures, including RMSE and MAPE [29].

4.2 Simulation parameters of networking modeling

Table 11 outlines key parameters for configuring traffic simulation software to model accurate traffic flow (Fig. 8(a) and (b)). Link lengths for all directions (West, South, East, North) remain constant at 12.00 PM and 4:30 PM, reflecting fixed distances in the simulation. Priority rules, including a 3-second minimum gap and 5-meter clearance, ensure safety and smooth traffic flow by preventing collisions and providing a buffer zone.

Table 11. Parameters used in VISSIM to create the simulation of the roundabout

12.00 p.m. scenario				
Parameters			**No**	
Link	West	South	East	North
	840 m	550 m	400 m	400 m
Circular link	60 m diameter			
Priority rule	Min gap time		Min clearance	
	3 s		5 m	
Data collection point	9.5 m distance from the circular link			
Queue counter	8.5 m distance from the circular link			
Detector	2 no, 5 m length each			
2-stage controller	5 m distance from the circular link			
4.30 p.m. scenario				
Parameters			**No**	
Link	West	South	East	North
	840 m	650 m	400 m	550 m
Circular link	60 m diameter			
	Min gap time		Min clearance	
Priority rule	3 s		5 m	
Data collection point	9.5 m distance from the circular link			
Queue counter	8.5 m distance from the circular link			
Detector	2 no, 5 m length each			
2-stage controller	5 m distance from the circular link			

The detector uses a small area detector to precisely monitor key points, such as intersection entries and exits, to gather accurate traffic flow data. The traffic light controller operates with a 2-stage system featuring balanced timings: 10 seconds for both green and red phases, a 1-second Red-Amber transition, a 3-second amber phase, and a 5-second clearance time. These settings ensure smooth transitions between phases and safe clearance before opposing traffic begins. Together, these parameters optimize traffic flow and contribute to a realistic, adjustable model for effective traffic management.

(a) (b)

Figure 8. Signalized Roundabout (a) 12.00 PM Scenario; (b) 4.30 PM Scenario

4.2 Statistical significance tests

Hypothesis testing for vehicular delay (Veh Delay) was conducted using a paired one-tailed t-test, comparing measurements before and after the intervention across four lanes. The null hypothesis (H_0) states that there is no significant difference in delays before and after detector placement, with a 95% confidence level and a 5% chance of error in the results ($\alpha = 0.05$). Since the p-value is less than α, the null hypothesis is rejected. The results are presented in Table 12.

Table 12. Statistical test of delay

12.00 p.m. scenario					
Lane	Before		After		p-value
	LOS	Veh delay	LOS	Veh delay	
West Lane	LOS_F	120.98	LOS_D	24.18	0.04
South lane	LOS_E	40.22	LOS_B	9.79	
East Lane	LOS_C	18.89	LOS_A	0.1	
North Lane	LOS_D	25.96	LOS_A	0.5	
4.30 p.m. scenario					
Lane	Before		After		p-value
	LOS	Veh delay	LOS	Veh delay	
West Lane	LOS_F	105.07	LOS_D	33.19	0.03
South lane	LOS_E	49.25	LOS_D	25.73	
East Lane	LOS_B	6.44	LOS_A	0.1	
North Lane	LOS_F	69.98	LOS_B	10.58	

The null hypothesis (H_0) for emissions in the paired one-tailed t-test states that there is no significant difference in emissions before and after detector placement, with a 95% confidence level and a 5% chance of error (α = 0.05). However, as shown in Table 13, the p-value is less than α, leading to rejecting the null hypothesis.

Table 13. Statistical test of emissions

12.00 p.m. scenario									
Lane	Before				After				p-value
	E [11] Co	E NOx	E Voc	FC [12]	E Co	E NOx	E Voc	FC	
West Lane	320.074	62.275	74.18	4.579	306.947	59.721	71.138	4.391	0.007
South lane	92.893	18.074	21.529	1.329	53.583	10.425	12.418	0.767	
East Lane	48.943	9.523	11.343	0.7	22.674	4.411	5.255	0.324	
North Lane	71.385	13.889	16.544	1.021	43.676	8.498	10.122	0.625	
4.30 p.m. scenario									
	Before				After				p-value
Lane	E Co	E NOx	E Voc	F C	E Co	E NOx	E Voc	FC	
West Lane	356.322	69.327	82.581	5.098	288.728	56.176	66.916	4.131	0.01
South lane	162.974	31.709	37.771	2.332	77.008	14.983	17.847	1.102	
East Lane	42.24	8.218	9.79	0.604	25.849	5.029	5.991	0.37	
North Lane	151.588	29.493	35.132	2.169	67.215	13.078	15.578	0.962	

11 = Emission, 12 = Fuel Consumption.

5. Discussion

5.1 Scenario- 12.00 PM

5.1.1 Optimal Queue Detector Location

Fig. 9 shows queue lengths for four lanes at various detector locations, with the south lane being signalized. The West Lane shows fluctuating queue lengths, with notable increases at 260 (251.22 m) and 300 (265.18 m), indicating potential congestion. The South Lane also fluctuates, with peaks at 250 (56.89 m), 260 (55.41 m), and 270 (57.04 m), suggesting varying congestion levels. The East Lane has low queue lengths, with occasional peaks at 250 (11.37 m) and 300 (5.03 m), and records 0 m at 240, 270, and 300, indicating free-flowing traffic. The North Lane remains relatively stable, with minor peaks at 240 (11.67 m), 250 (11.58 m), and 270

(13.78 m), experiencing minimal congestion. The analysis confirms that the optimal detector location is at 240 m in the signalized south approach.

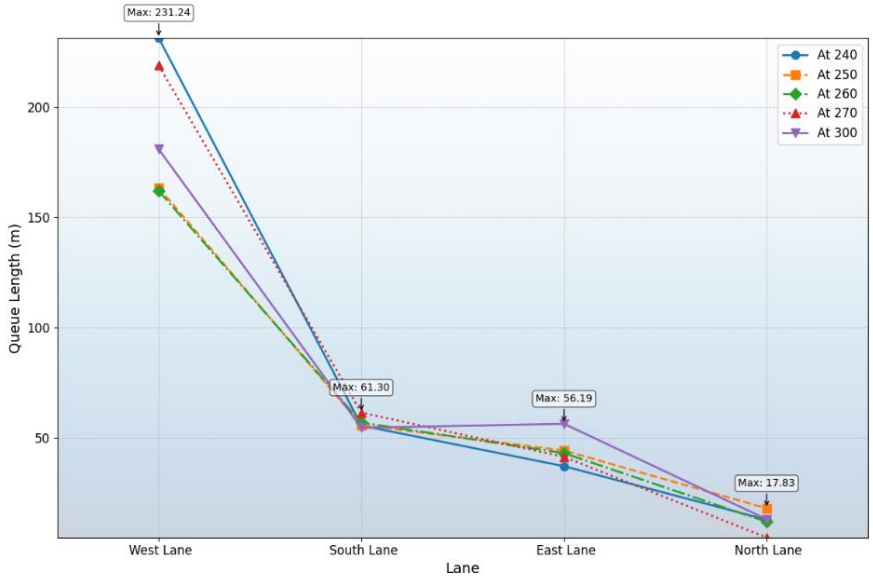

Figure 9. South approach signalized

5.1.2 Comparison of Level of Service (LOS)

Fig. 10 compares the Level of Service (LOS) and vehicle delays before and after traffic signal implementation, highlighting its impact on traffic conditions. The West Lane improved from LOS_F with a high vehicle delay of 120.98 sec to LOS_D and a delay of 24.18 sec, reflecting reduced congestion. The South Lane improved from LOS_E (40.22 sec delay) to LOS_B (9.79 sec). The East Lane showed the most significant improvement, from LOS_C (18.89 seconds delay) to LOS_A (0.1 seconds). The North Lane improved from LOS_D (25.96 sec) to LOS_A (0.5 seconds). These results align with studies by Othayoth et al. [30] and Alkaissi et al. [31], validating the signal's positive impact on traffic flow and delay reduction.

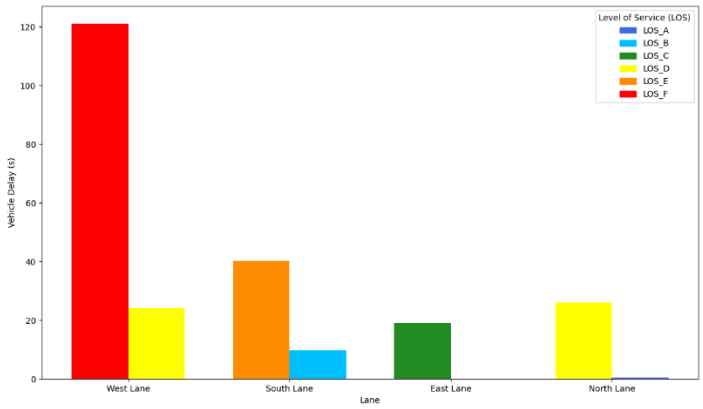

Figure 10. LOS & Vehicle delay before and after the signal was implemented

5.1.3 comparison of emissions

Fig. 11(a) and (b) compare emissions and fuel consumption across four lanes before and after signal implementation. Before the signal, the West Lane had the highest emissions (CO, NOX, VOC) and fuel consumption, indicating a significant environmental burden. The South Lane showed lower emissions than the West Lane but contributed notably to pollution. The East Lane had the lowest emissions, reflecting cleaner,

more fuel-efficient traffic. The North Lane had moderate emissions, higher than the East Lane but lower than the West and South lanes. Post-signal, the West Lane continued to show the highest emissions, while the South Lane's emissions decreased, indicating improved environmental impact. The East Lane maintained the lowest emissions, and the North Lane showed controlled moderate emissions. These results align with studies by Kwak et al. [32] and Zhang et al. [33] on the benefits of signal optimization in reducing emissions and fuel consumption.

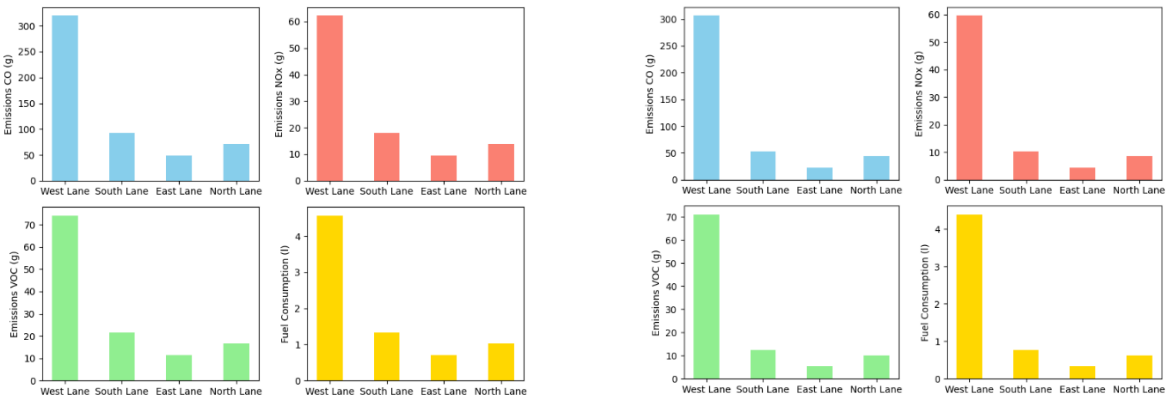

Figure 11. Emissions of roundabout (a) before and (b) after signal implemented

5.2 Scenario- 4.30 PM

5.2.1. Queue detector location

Fig. 12 shows queue lengths for six detector locations based on the south lane being signalized. The West Lane's queue length fluctuates between 107.93 m and 216.51 m, with temporary relief at 350 and 500-time points and congestion resurgence at 550. The South Lane shows an increasing trend in queue length from 75.77 m to 100.22 m, indicating growing congestion from 300 to 550 time points. The East Lane experiences low and stable queue lengths, ranging from 6 to 16.98 m, suggesting minimal congestion. The North Lane shows relatively stable congestion, with 34.79 m and 55.19 m queue lengths. These stability patterns align with Wu and Yang [34], who noted lower fluctuation in lanes with consistent flow. Based on the analysis, 350 meters is the ideal detector location, consistent with Chang et al. [35], who highlighted the importance of optimal detector placement for accurate queue length estimation.

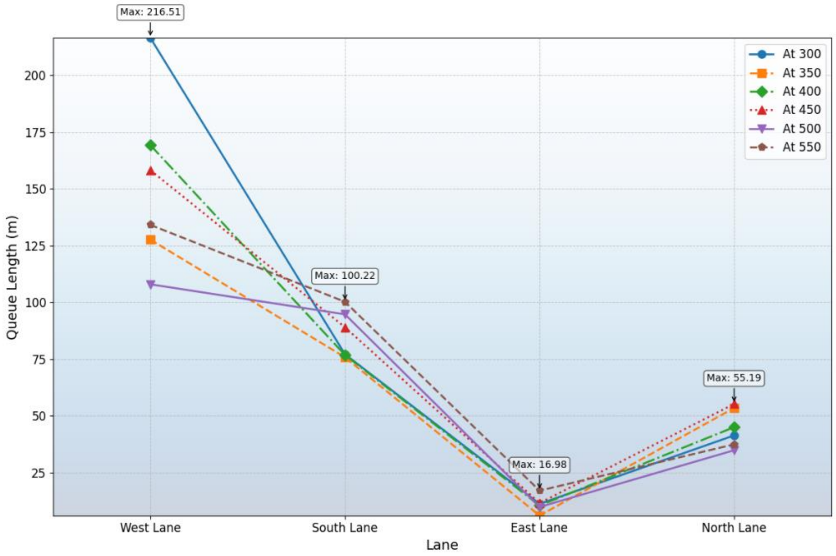

Figure 12. South approach signalized

5.2.2 Comparison of LOS & vehicle delay

Fig. 13 shows that signal implementation significantly improved traffic performance across all lanes, as reflected by Level of Service (LOS) and vehicle delay metrics.

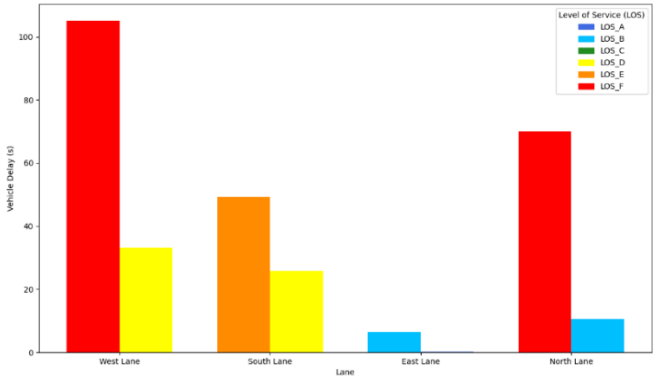

Figure 13. LOS & Vehicle delay before and after the signal was implemented

Gopalakrishnan et al.[36] Confirm that signal improvements enhance intersection efficiency, as measured by delays and LOS grades. Before the signal, the West Lane had severe congestion (LOS F, 105.07 seconds delay), which improved to LOS D and a 33.19-second delay. The South Lane improved from LOS E (49.25 seconds delay) to LOS D (33.73 seconds). The East Lane, already performing well (LOS B, 6.44 seconds delay), improved to LOS A with a negligible 0.1-second delay. The North Lane dramatically improved from LOS F (69.98 seconds) to LOS B (10.58 seconds). Saha et al.[37] highlight the importance of accounting for lane performance variation during signal optimization. These results demonstrate the signal's effectiveness in reducing congestion and optimizing traffic flow.

5.2.3 comparison of emissions

Fig. 14(a) shows emissions and fuel consumption across four lanes before signalization. The West Lane has high emissions (CO: 356.322, NOx: 69.327, VOC: 82.581 units) and fuel consumption (5.098 units), indicating a significant environmental impact. The South Lane has lower emissions (CO: 162.974, NOx: 31.709, VOC: 37.771) and fuel consumption (2.332 units). The East Lane exhibits minimal emissions (CO: 42.24, NOx: 8.218, VOC: 9.79) and fuel consumption (0.604 units), suggesting cleaner conditions. The North Lane has moderate emissions (CO: 151.588, NOx: 29.493, VOC: 35.132) and fuel consumption (2.169 units). After signalization (Fig. 14(b)), the West Lane still has high emissions (CO: 288.728, NOx: 56.176, VOC: 66.916) and fuel consumption (4.131 units).

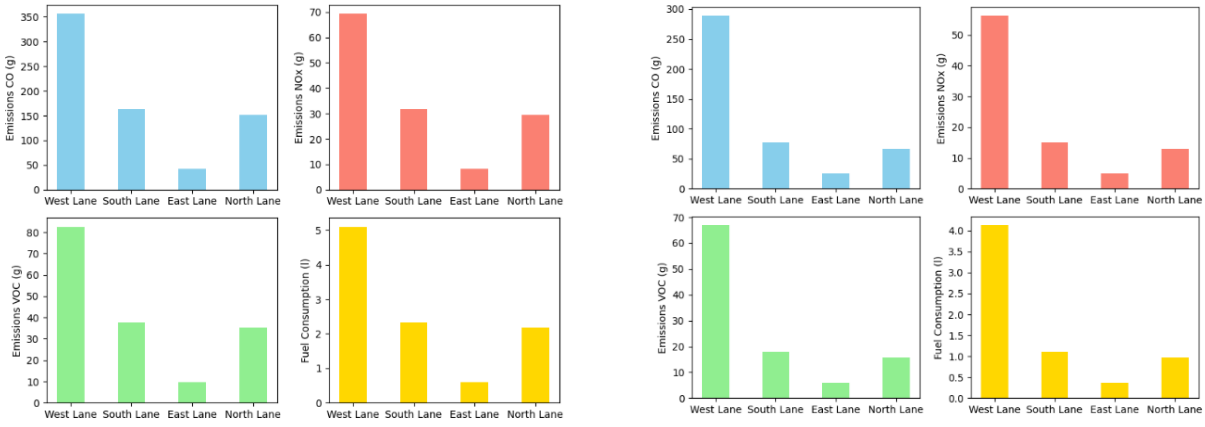

(a) (b)

Figure 14. Emissions of roundabout (a) before and (b) after signal implemented

The South Lane shows reduced emissions (CO: 77.008, NOx: 14.983, VOC: 17.847) and fuel consumption (1.102 units), indicating improved environmental conditions. The East Lane shows minimal emissions (CO: 25.849, NOx: 5.029, VOC: 5.991) and low fuel consumption (0.37 units), demonstrating efficient traffic flow. The North Lane has moderate emissions (CO: 67.215, NOx: 13.078, VOC: 15.578) and fuel consumption (0.962 units). These results align with Li and Sun [38], showing that signal optimization reduces environmental impact and improves traffic performance.

6. Conclusion

In urban transportation systems, effectively managing traffic flow, particularly in areas with both roundabouts and signal-controlled intersections, is crucial. This study presents key findings from various scenarios simulated using VISSIM software, focusing on the impact of implementing signal controls on traffic flow dynamics and Level of Service (LOS) across different lanes.

During the 4:30 PM scenario, the roundabout experienced severe congestion, particularly in the North and West Lanes, both rated as LOS F. Introducing a signal at the South Lane significantly improved conditions, leading to LOS D and LOS B for the West and North Lanes, respectively, especially at the 240-meter detector point. Similarly, in the 12:00 PM scenario, West Lane initially faced LOS F conditions. Implementing signal controls at the 350-meter detector location in this scenario also resulted in notable improvements: the West Lane experienced slightly reduced emissions and fuel consumption; the South Lane's emissions were significantly reduced; the East Lane maintained the lowest emissions; and the North Lane showed moderate emissions with a controlled environmental impact. For the 4:30 PM scenario, the West Lane still exhibited higher emissions and fuel consumption than other lanes, while the South Lane showed reduced emissions and fuel consumption. The East Lane continued to demonstrate minimal emissions and fuel consumption, and the North Lane's emissions were comparable to those of the South Lane, with moderate fuel consumption.

Overall, the study demonstrates that the strategic implementation of signal controls can significantly enhance traffic flow and reduce environmental impacts in congested urban areas.

7. Limitation

A limitation of this study was the use of a student version of VISSIM, restricting signal control to a 2-stage system and limiting the exploration of advanced strategies. Additionally, the study did not account for noise pollution impacts, which are crucial for comprehensively evaluating transportation systems. Furthermore, the life cycle assessment (LCA) was limited, potentially overlooking significant environmental impacts over the entire lifespan of the transportation infrastructure. Lastly, the study did not incorporate comprehensive sustainability metrics, which are essential for evaluating the proposed solutions' long-term viability and environmental impact.

8. Future research directions

Future research could use licensed VISSIM or SUMO and explore advanced signal controllers like adaptive or actuated systems for better traffic management insights. Additionally, future studies should include the assessment of noise pollution impacts to provide a more comprehensive evaluation of transportation systems. Expanding the scope of life cycle assessments (LCA) to cover the entire lifespan of transportation infrastructure is also recommended to ensure all significant environmental impacts are considered. Incorporating comprehensive sustainability metrics will be essential for evaluating proposed solutions' long-term viability and environmental impact. These additions will help create a more holistic understanding of the effects of transportation systems on urban environments.

9. Acknowledgements

The authors wish to extend their sincere gratitude to the anonymous reviewers for their insightful comments and constructive feedback. Their thorough evaluation and valuable suggestions have significantly enhanced the quality and clarity of this manuscript.

Author Contributions: M.H: Writing – original draft, Software, Resources, Methodology, Funding acquisition, Formal analysis, Data curation, Conceptualization. H.K.A: Writing – review & editing, Supervision, Conceptualization. H.D.M: Writing – review & editing, Software, Visualization, Validation, Resources, Formal analysis. A.A.N: Writing – review & editing. S.S.S: Writing – review & editing. A.P: Writing – review & editing.

Funding: This research received no external funding.

Conflicts of Interest: The authors declare that there is no conflict of interest regarding the publication of this paper.

References

[1] United Nations https://www.un.org/development/desa/en/news/population/2018-revision-of-world-urbanization-prospects.html (accessed August 28, 2024).

[2] Angel, S.; Parent, J.; Civco, D. L.; Blei, A.; Potere, D. The Dimensions of Global Urban Expansion: Estimates and Projections for All Countries, 2000–2050. *Prog Plann*, **2011**, *75*(2), 53–107. https://doi.org/10.1016/j.progress.2011.04.001.

[3] Kundu, D.; Pandey, A. K. World Urbanisation: Trends and Patterns. *Developing national urban policies: Ways forward to green and smart cities*, **2020**, 13–49. https://doi.org/10.1007/978-981-15-3738-72.

[4] HARVARD T.H CHAN https://www.hsph.harvard.edu/news/hsph-in-the-news/air-pollution-traffic-levy-von-stackelberg/ (accessed August 28, 2024).

[5] World Health Organization REGIONAL OFFICE FOR Europe https://who-sandbox.squiz.cloud/en/health-topics/environment-and-health/air-quality/data-and-statistics (accessed August 28, 2024).

[6] Akçelik, R. Roundabouts with Unbalanced Flow Patterns. In *ITE 2004 Annual Meeting*, **2004**, 41.

[7] Martin-Gasulla, M.; García, A.; Moreno, A. T. Benefits of Metering Signals at Roundabouts with Unbalanced Flow: Patterns in Spain. *Transp Res Rec*, **2016**, *2585*(1), 20–28. https://doi.org/10.3141/2585-03.

[8] Duan, Y.; Qu, X.; Easa, S.; Yan, Y. Optimising Total Entry Delay at Roundabouts with Unbalanced Flow: A Dynamic Strategy for Smart Metering. *IET Intelligent Transport Systems*, **2019**, *13*(3), 485–494.

[9] An, H. K.; Bae, G.; Kim, D. S. Study of Full Controlled Green Time Roundabouts–An Intelligent Approach. *Promet-Traffic&Transportation*, **2023**, *35*(2), 212–229.

[10] Akçelik, R. Capacity and Performance Analysis of Roundabout Metering Signals. In *TRB National Roundabout Conference, Vail, Colorado, USA*; 2005, 22–25.

[11] Akçelik, R. Roundabout Metering Signals: Capacity, Performance and Timing. *Procedia-Social and Behavioral Sciences*, **2011**, *16*, 686–696. https://doi.org/10.1016/j.sbspro.2011.04.488.

[12] Martin-Gasulla, M.; Garcia, A.; Moreno, A. T.; Llorca, C. Capacity and Operational Improvements of Metering Roundabouts in Spain. *Transportation research procedia*, **2016**, *15*, 295–307. https://doi.org/10.1016/j.trpro.2016.06.025.

[13] Sun, X.; Ma, W.; Huang, W. Comparative Study on the Capacity of a Signalised Roundabout. *IET Intelligent Transport Systems*, **2016**, *10*(3), 175–185. https://doi.org/10.1016/j.trpro.2016.06.025

[14] Adegbaju, O. A. Establishing Delay-Based Criteria for Installing Traffic Signals at Two-Lane Roundabouts. **2018**.

[15] An, H. K.; Yue, W. L.; Stazic, B. Estimation of Vehicle Queuing Lengths at Metering Roundabouts. *Journal of Traffic and Transportation Engineering (English Edition)*, **2017**, *4*(6), 545–554. https://doi.org/10.1016/j.jtte.2017.04.002.

[16] An, H. K.; Abdalla, A. N. Prediction of Queuing Length at Metering Roundabout Using Adaptive Neuro Fuzzy Inference System. *Measurement and Control*, **2019**, *52*(5–6), 432–440. https://doi.org/10.1177/0020294019839415.

[17] Osei, K. K.; Adams, C. A.; Ackaah, W.; Oliver-Commey, Y. Signalization Options to Improve Capacity and Delay at Roundabouts through Microsimulation Approach: A Case Study on Arterial Roadways in Ghana. *Journal of Traffic and Transportation Engineering (English Edition)*, **2021**, *8*(1), 70–82. https://doi.org/10.1016/j.jtte.2019.06.003.

[18] Vichova, K.; Heinzova, R.; Dvoracek, R.; Tomastik, M. Optimization of Traffic Situation Using Roundabouts. *Transportation research procedia*, **2021**, *55*, 1244–1250. https://doi.org/10.1016/j.trpro.2021.07.106.

[19] An, H. K.; Liu, Y.; Kim, D. S. Operational Optimization at Signalized Metering Roundabouts Using Cuckoo Search/Local Search Algorithm. *Measurement and Control*, **2022**, *55*(9–10), 1110–1123. https://doi.org/10.1177/00202940221101895.

[20] Kabit, M. R.; Chiew, W. Y.; Chai, A.; Tirau, L. S.; Bujang, Z. Evaluating the Effects of Signal Control Applications on Roundabout's LOS Performance Using VISSIM Microsimulation Model. *International Journal of Integrated Engineering*, **2023**, *15*(6), 13–22. https://doi.org/10.30880/ijie.2023.15.06.002.

[21] Assolie, A. A.; Sukor, N. S. A.; Khliefat, I.; Abd Manan, T. S. B. Modeling of Queue Detector Location at Signalized Roundabouts via VISSIM Micro-Simulation Software in Amman City, Jordan. *Sustainability*, **2023**, *15*(11), 8451. https://doi.org/10.3390/su15118451

[22] Abdullah, M. S.; Sanik, M. E.; Nor, A. H. M.; Salim, S.; Malek, K. Z. A.; Razali, N. F.; Nasir, A. Z. M. Reliability of 15-Minute Drone Footage Volume for Estimating Urban Traffic Flow Rates: A Preliminary Study. In *IOP Conference Series: Earth and Environmental Science*; IOP Publishing, **2022**, 1022, 012022.

[23] Du, Y.; Zhao, C.; Li, F.; Yang, X. An Open Data Platform for Traffic Parameters Measurement via Multirotor Unmanned Aerial Vehicles Video. *J Adv Transp*, **2017**, *2017*(1), 8324301. https://doi.org/10.1155/2017/8324301.

[24] Lee, M.-Y.; Park, J.-J.; Jin, T.-H.; Ha, T.-J. Establishment of Traffic Information Image Collection System Using Drones. *KSCE Journal of Civil and Environmental Engineering Research*, **2020**, *40*(4), 401–408. https://doi.org/10.12652/Ksce.2020.40.4.0401.

[25] Krogscheepers, J. C.; Roebuck, C. S. Unbalanced Traffic Volumes at Roundabouts. In *Fourth International Symposium on Highway Capacity, Transportation Research Circular E-C018*, **2000**, 446–458.

[26] Assolie, A. A.; Sukor, N. S. A.; Khliefat, I.; Abd Manan, T. S. B. Modeling of Queue Detector Location at Signalized Roundabouts via VISSIM Micro-Simulation Software in Amman City, Jordan. *Sustainability*, **2023**, *15*(11), 8451. https://doi.org/10.3390/su15118451.

[27] Rathnayake, I.; Amarasinghe, N.; Wickramasinghe, V.; Liyanage, K. Queue Length Prediction at Un-Signalized Intersections with Heterogeneous Traffic Conditions. **2022**. http://rda.sliit.lk/handle/123456789/3005.

[28] Kan, X. D.; Ramezani, H.; Benekohal, R. F. *Calibration of VISSIM for Freeway Work Zones with Time-Varying Capacity*; 2014.

[29] Mehar, A.; Chandra, S.; Velmurugan, S. Highway Capacity through Vissim Calibrated for Mixed Traffic Conditions. *KSCE journal of Civil Engineering*, **2014**, *18*, 639–645. https://doi.org/10.1007/s12205-014-0440-3.

[30] Othayoth, D.; Rao, K. V. K.; Bhavathrathan, B. K. Perceived Level of Service at Signalized Intersections under Heterogeneous Traffic Conditions. *Transportmetrica A: transport science*, **2020**, *16*(3), 1294–1309. https://doi.org/10.1080/23249935.2020.1737270.

[31] Alkaissi, Z. A. Effect of Signal Coordination on the Traffic Operation of Urban Corridor. *Tikrit Journal of Engineering Sciences*, **2023**, *30*(1), 12–24. http://doi.org/10.25130/tjes.30.1.2.

[32] Kwak, J.; Park, B.; Lee, J. Evaluating the Impacts of Urban Corridor Traffic Signal Optimization on Vehicle Emissions and Fuel Consumption. *Transportation Planning and Technology*, **2012**, *35*(2), 145–160. https://doi.org/10.1080/03081060.2011.651877.

[33] Zhang, X.; Fang, S.; Shen, Y.; Yuan, X.; Lu, Z. Hierarchical Velocity Optimization for Connected Automated Vehicles with Cellular Vehicle-to-Everything Communication at Continuous Signalized Intersections. *IEEE Transactions on Intelligent Transportation Systems*, **2023**, *25*(3), 2944–2955. https://doi.org/10.1109/TITS.2023.3274580.

[34] Wu, A.; Yang, X. Real-Time Queue Length Estimation of Signalized Intersections Based on RFID Data. *Procedia-Social and Behavioral Sciences*, **2013**, *96*, 1477–1484. https://doi.org/10.1016/j.sbspro.2013.08.168.

[35] Chang, J.; Talas, M.; Muthuswamy, S. Simple Methodology for Estimating Queue Lengths at Signalized Intersections Using Detector Data. *Transp Res Rec*, **2013**, *2355*(1), 31–38. https://doi.org/10.3141/2355-04.

[36] Gopalakrishnan, A.; Ram, S.; Sarkar, P. K. Development of Composite Level of Service for Signalized Intersections Under Heterogeneous Traffic Conditions. *Transportation in Developing Economies*, **2019**, *5*(2), 19. https://doi.org/10.1007/s40890-019-0087-3.

[37] Saha, A.; Chandra, S.; Ghosh, I. Assessment of Level of Service for Urban Signalized Intersections in India. *Curr Sci*, **2019**, *117*(9), 1516–1521. https://www.jstor.org/stable/27138489.

[38] Li, X.; Sun, J.-Q. Turning-Lane and Signal Optimization at Intersections with Multiple Objectives. *Engineering Optimization*, **2019**, *51*(3), 484–502. https://doi.org/10.1080/0305215X.2018.1472250.